

Experimental Investigation for Enhancement of Heat Transfer in Double Pass Solar Air Heater Using Transverse Discrete Rib Geometry

ANKUR VISHWAKARMA*, Dr. A. R. JAURKER**

*Researcher, Department Of Mechanical Engineering, Jabalpur Engineering College
Jabalpur.

**Professor, Department Of Mechanical Engineering, Jabalpur Engineering College
Jabalpur.

ABSTRACT

An important and attractive design improvement over conventional single pass solar air heater to increase its thermal performance is the Double pass solar air heater. This paper presents an experimental study to investigate the effect of roughness and flow parameters on heat transfer using transverse rib geometry. The investigation has covered the range of Reynolds number 2000 to 14000, relative roughness pitch 6 to 12 for constant relative roughness height of 0.028. Collected data has been compared with those of smooth duct under similar operating condition. Results reveal an enhancement of 3.6 times in Nusselt number compare to smooth duct.

Key words: Double pass, Artificial Roughness, Heat Transfer, Nusselt Number, Friction Factor.

1. INTRODUCTION

Various configuration of Solar Air Heater (SAHs), have been made available in literature by investigators to study the enhancement of convective heat transfer coefficient [1-6]. A number of alternative designs have been proposed over the conventional Single Pass Solar Air Heater. These designs must be able to reduce heat losses from the collector, so as to increase operating temperature and system efficiency. For this Double pass solar air heater has been introduced. In the double pass arrangement collector consists of two passages; first passage is formed between the two glass covers and the second passage where in air flows in the reverse direction is formed between the absorber plate and the wooden duct. This increases the thermal energy between the absorber plate and the air, which clearly improves the thermal performances of the solar collectors with obstacles arranged into the air channel duct [7, 8].

Mohamad [9], carried out a simulation study of a double-pass solar collector with porous media aiming to minimize heat losses from the front cover of the collector and to maximize heat extraction from the heated wall (absorber). This objective can be achieved by forcing air

to flow through first pass (pre-heat the air) before passing through the second pass. In designing this type of collector, which combines double air passage and porous media, pressure drop should be minimized. However, the thermal efficiency of this type of collector is significantly higher than the thermal efficiency of conventional air heaters, exceeding 75% under normal operating conditions. The pressure drop is not so significant if high porous medium is used and careful design of U-return section is considered.

Ramadan et al. [10], experimentally investigated the thermal performance of a double-glass double-pass solar air heater with a packed bed (DPSAHPB) above the heater absorber plate. Limestone and gravel were used as packed bed materials. Numerical calculations were carried out, to study the effect of different operational and configurationally parameters on the heater performance. Effects of the mass flow rate of air and the mass and porosity of the packed bed material were also studied. It was inferred that for increasing the outlet temperature to of the flowing air after sunset, it is advisable to use the packed bed materials with higher masses and therefore with low porosities. It is recommended to operate the system with packed bed with values of equal 0.05 kg/s or lower to have a lower pressure drop across the system.

Apart from using porous materials such stones, crushed glass, wool as heat absorbing materials addition ribs of various cross sections such as square, rectangular, semicircular and circular, various shapes (transverse, transverse discrete, multiple V, V down inclined etc.) and pitch on the underside of the plate also fulfills the same purpose [11-15]. It hinders the formation of laminar sub layer, results in increase of heat transfer coefficient.

Prasad and Saini [16, 17], studied the effect of roughness and flow parameters such as relative roughness height (e/D) and relative roughness pitch (p/e) on heat transfer and friction factor using transverse continuous ribs. Expressions were also being developed for the heat transfer and friction factor for a fully turbulent flow. It was observed that maximum heat transfer occurred in the vicinity of reattachment points and reattachment of free shear layer does not occur if relative roughness pitch (P/e) is less than about 8 to 10. Optimal thermo hydraulic performance is achieved for roughness height slightly higher than the transition sub layer thickness. For relative roughness height (e/D) value of 0.033 and relative roughness pitch (p/e) value of 10, maximum enhancement in Nusselt number and friction factor was reported to be 2.38 and 4.25 times respectively over smooth duct.

Sahu and Bhagoria [18], investigated the effect of 90° broken ribs on thermal performance of a SAH for fixed roughness height (e) value of 1.5 mm, duct aspect ratio (W/H) value of 8, pitch (p) in the range of 10–30 mm and Reynolds number (Re) range of 3000–12,000. Roughened absorber plate increased the heat transfer coefficient by 1.25 to 1.4 times as compared to smooth one under similar operating conditions. Corresponding to roughness pitch (p) value of 20 mm, maximum value of Nusselt number was obtained that decreased on the either side of it. The thermal efficiency of roughened solar air heater was found to be in the range of 51–83.5% depending upon the flow conditions.

The objective of the present investigation is to generate heat transfer data pertinent to the heating of air in a double pass rectangular duct with transverse discrete repeated rib roughness on one broad heated wall (absorber plate) for varying range of Reynolds number and other operating parameters.

2. ROUGHNESS GEOMETRY AND RANGE OF PARAMETERS

The roughness parameters are determined by rib height (e), rib and pitch (p). These parameters have been expressed in the form of the following dimensionless variables as:

- (a) **Shape of roughness element:** The roughness element may be two-dimensional ribs or three dimensional either transverse or inclined of any special form. The common shape of roughness element is square, circular, semi-circular, chamfered, arc shaped wire; dimple or cavity, compound rib-grooved and v-shaped continuous or broken ribs with or without gap can be considered to investigate the thermo hydraulic performance of the solar air heater duct.
- (b) **Relative roughness pitch (P/e):** It is the ratio of distance between two consecutive ribs and height of the rib.
- (c) **Relative roughness height (e/D):** It is the ratio of rib height to equivalent diameter of the air passage.
- (d) **Angle of attack (α):** Angle of attack is defined as the inclination of rib with direction of air flow in the duct.
- (e) **Aspect ratio (W/H):** Aspect ratio is defined as the ratio of duct width to duct height. This factor also plays a very crucial role in investigating thermo-hydraulic performance.

Range of parameters and rib geometry is shown below in table 1 and fig 1 respectively.

Table1. Range of parameters

Reynolds number (Re)	3000 - 18000
Relative roughness pitch(P/e)	6 to 12
Relative roughness height(e/D)	0.028
Angle of attack (α)	90°
Aspect ratio(W/H)	6.67

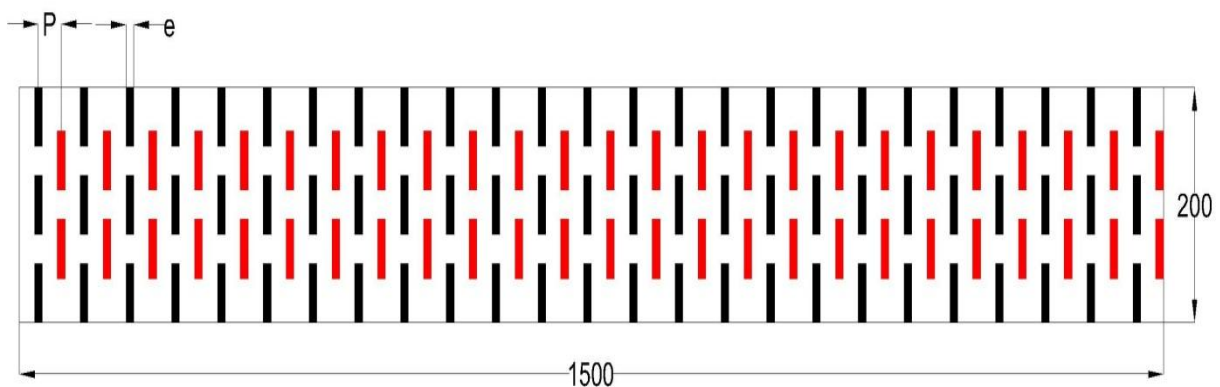


Fig. 1. Roughness Geometry

3. EXPERIMENTAL PROGRAM

3.1 Experimental apparatus

The schematic diagram of experimental set up is shown in Fig. 2(a) and 2(b). The experimental set up has been designed, fabricated and tested for data collection.

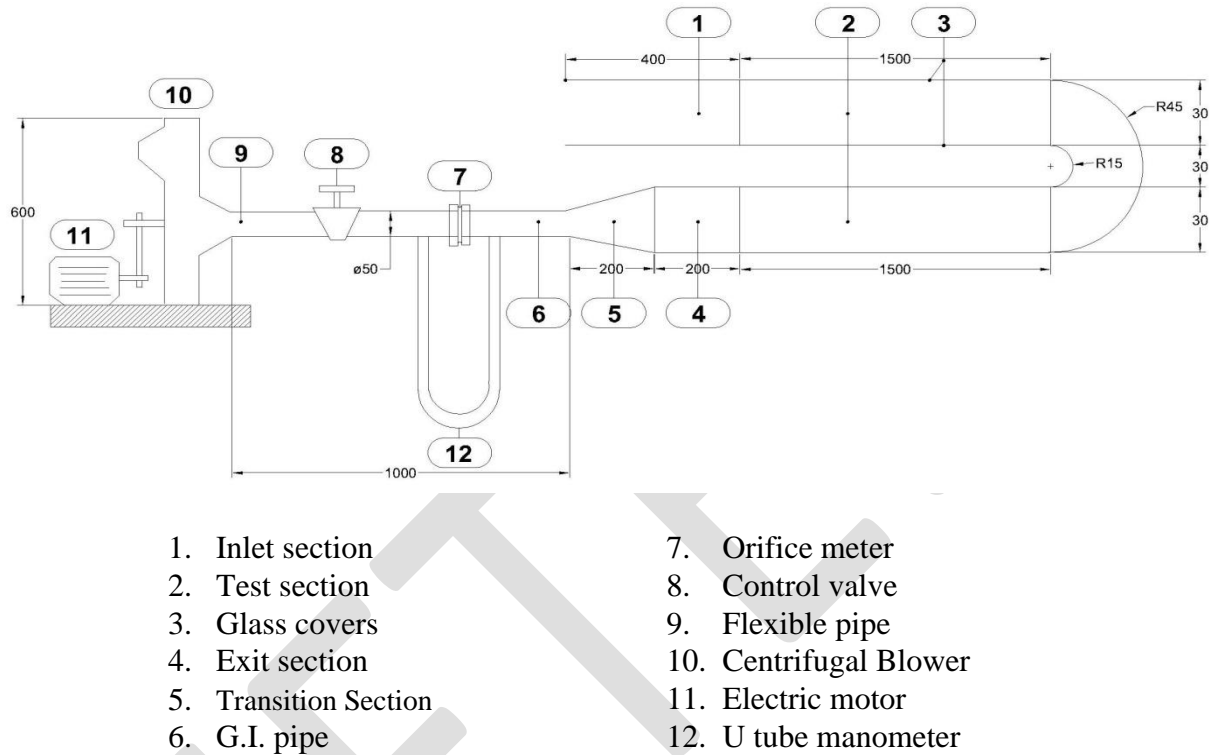


Fig .2 (a). Experimental Set-Up (all dimensions are in mm)

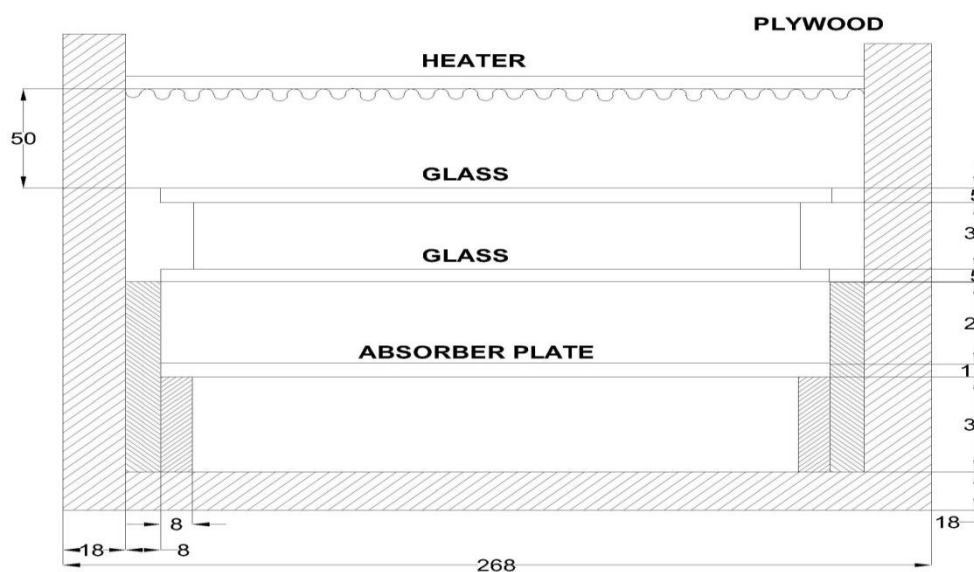


Fig .2 (b). Cross Sectional View (all dimensions are in mm)

In the double pass arrangement collector consists of two passages; first passage is formed between the two glass covers and the second passage where in air flows in the reverse direction is formed between the absorber plate and the lower wooden duct. Both the passages have identical length of 1500 mm, width of 400 mm and depth 30 mm. Transparent glass cover of 5.0 mm thickness is fitted above the absorber plate at a gap of 30.0 mm with the help of batons and rubber packing fixed adjacent to the sidewalls. Another glass cover of similar size is kept at a distance of 30.0 mm above the first glass cover. Two passages are connected by a smooth U-turn made up of G.I. sheet and insulated to avoid heat losses to the surroundings. Sides of both the solar collectors are made up of 18.0 mm thick wood to reduce heat losses to the surroundings.

Entrance and exit duct have been provided at the inlet and outlet of the test collectors to stabilize the air flow. These are made from plywood of thickness 18.0 mm and having the same cross section as that of test section. The length of entry and exit section has been taken as 400 mm and 200 mm respectively. This has been decided based on the recommendation of [ASHRAE Standard 92-77 \(1997\)](#). The exit section is connected to blower through a G.I pipe, a transition piece and flexible pipes. A centrifugal blower of 2.2 kW (2.0 h.p) capacity, driven by a 3-phase 440V, 2.3kW and 1420 rpm A.C. motor has been used to draw the ambient air into the collector through the entrance section. An electrical heater of size 1500 mm × 200 mm is fabricated by nichrome wire as desired requirement radiating uniform heat flux of 1000 W/m².

Measurement of mass flow rate of air through each collector has been accomplished by a separate calibrated 25 mm diameter orifice plate. Temperatures at different points along the length of absorber plate and air at different locations as shown in the following figure have been measured with the help of k -type thermocouple. A digital multi - meter is used to indicate the output of the thermocouples through the selector switch.

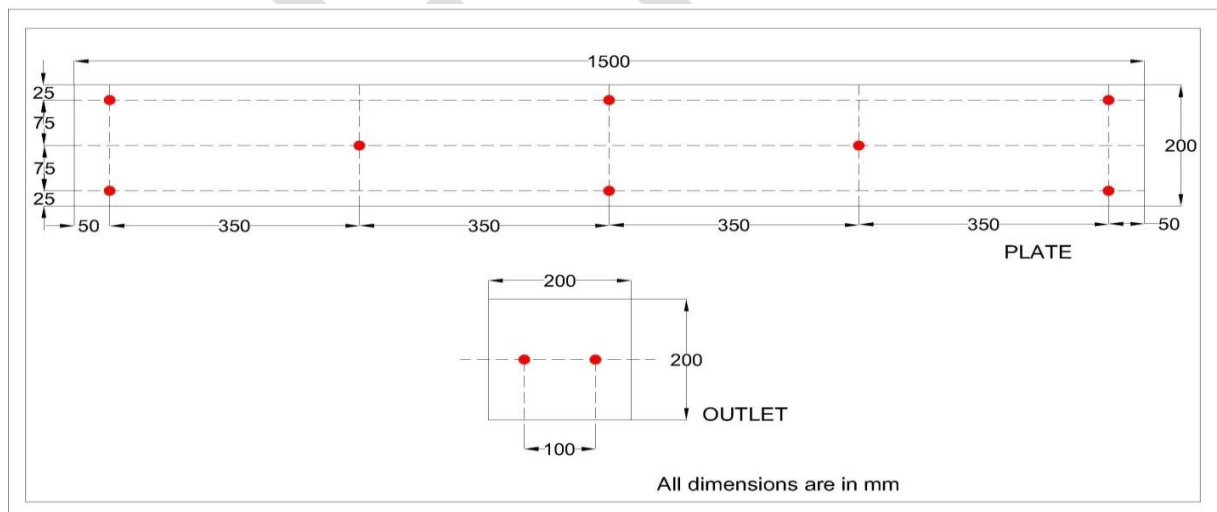


Fig. 3. Position of thermocouples

3.2 Absorber Plate

A 1.2 mm thick G.I. absorber plate have been prepared by pasting circular wires (ribs) of 1.5 mm diameter on the face opposite to the one facing solar radiation. Ribs were placed considering different values of pitch at an angle of attack of 90° as shown in figure 1. It was

blackened with blackboard paint on the side facing solar radiation. Below the absorber plate plywood of 18.0 mm thickness, followed by 25.0 mm thick rock wool have been placed. This has been done to prevent the heat loss to the surroundings from the bottom of the collector.

3.3 Experimental procedure

The test runs to collect relevant heat transfer were conducted under quasi-steady state conditions. The quasi-steady state condition was assumed have to been reached when the temperature at the point does not change for about 10 minutes. When a change in the operating conditions is made, it takes about 30 min to reach such a quasi-steady state. Seven values of flow rates were used for each set at a constant heat flux of the test. After each of flow rate, the system is allowed to attain a steady state before the data were recorded.

The following parameters were measured:

1. Temperature of heated plate
2. Temperature of air at inlet and outlet of the test section
3. Pressure difference across orifice meter

4. DATA REDUCTION

Under steady state condition with the help of below mentioned formulas useful parameters were being calculated. Mass flow rate (\dot{m}), heat supplied to the air (q), heat transfer coefficient (h), was calculated as:

$$\dot{m} = cd A_o \sqrt{\frac{2\rho(\delta P)}{1-\beta^4}} \quad (1)$$

$$Q_{air} = \dot{m} c_p (T_o - T_i) \quad (2)$$

$$h = \frac{Q_{air}}{A_p (T_p - T_f)} \quad (3)$$

where the temperature T_p and T_f are the average absorber plate and fluid temperature respectively. The plate temperature was determined at eight points of the absorber plate as shown in figure 3.

The convective heat transfer coefficient has been used to determine the Nusselt number as

$$N_u = \frac{h D_h}{k} \quad (4)$$

Thermal efficiency is calculated using following formula

$$\eta = \frac{G C_p (T_o - T_i)}{I} \quad (5)$$

$$G = \frac{\dot{m}}{A_p} \quad (6)$$

Where G = mass velocity, A_p = area of the plate, I = heat flux

5. VALIDITY TEST

Prior to actual data collection, the test set up was checked by conducting experiments for smooth duct. The Nusselt number determined from these experimental data for smooth duct have been compared with the values obtained from correlation for the Nusselt number. The result obtained is shown in figure 4.

$$Nu = 0.023Re^{0.8}Pr^{0.4}$$

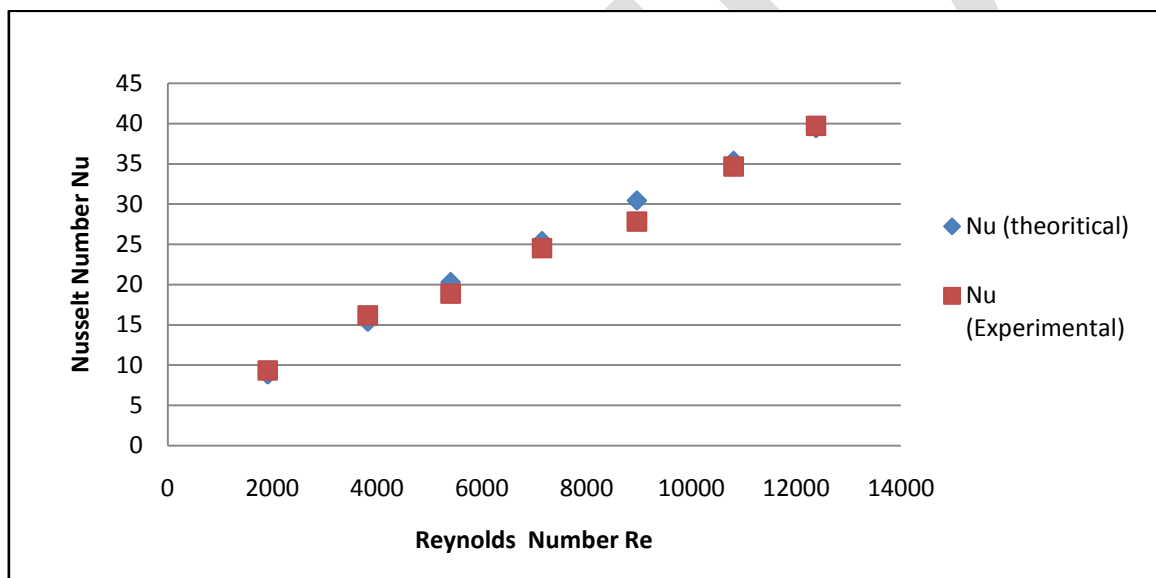


Fig .4. Nusselt Number Vs Reynolds Number With for Smooth Duct

6. RESULTS AND DISCUSSION

The effect of various flow and roughness parameter on heat transfer characteristics for air flowing through a rectangular cross section double pass solar air heater duct is shown below. In each graph comparison between roughened duct and smooth duct is made to determine the enhancement in heat transfer.

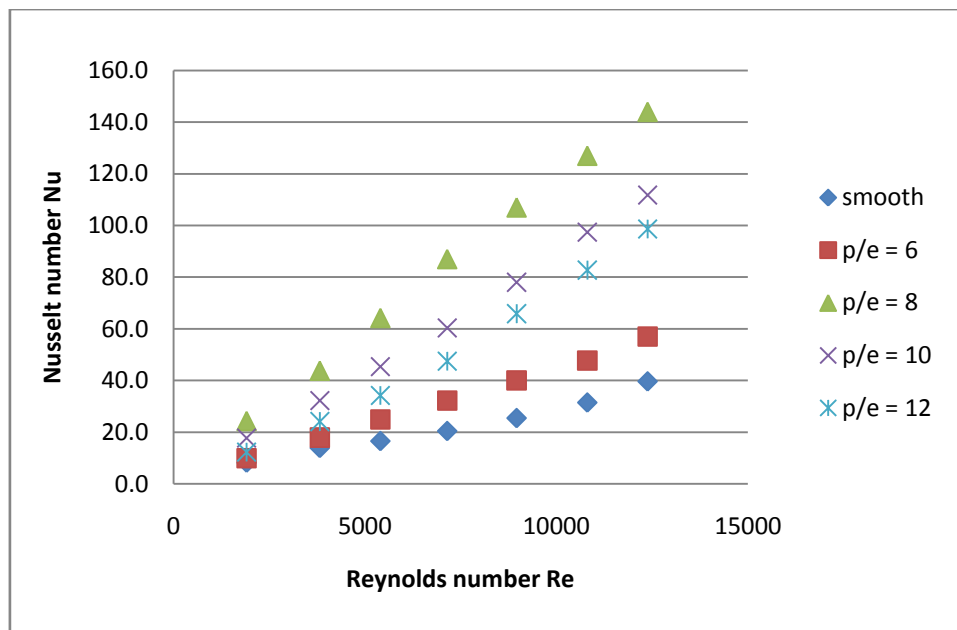


Fig .5. Nusselt Number Vs Reynolds Number for Different Relative Roughness (P/e)

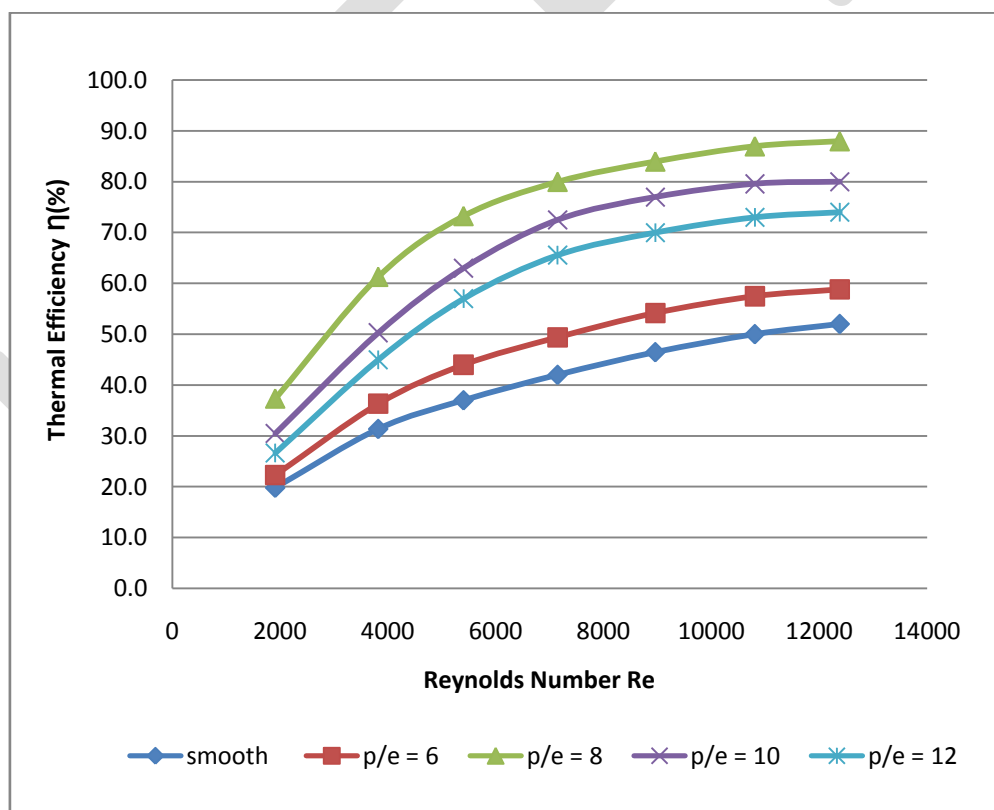


Fig. 6. Thermal Efficiency Vs Reynolds Number for Different Relative Roughness (P/e)

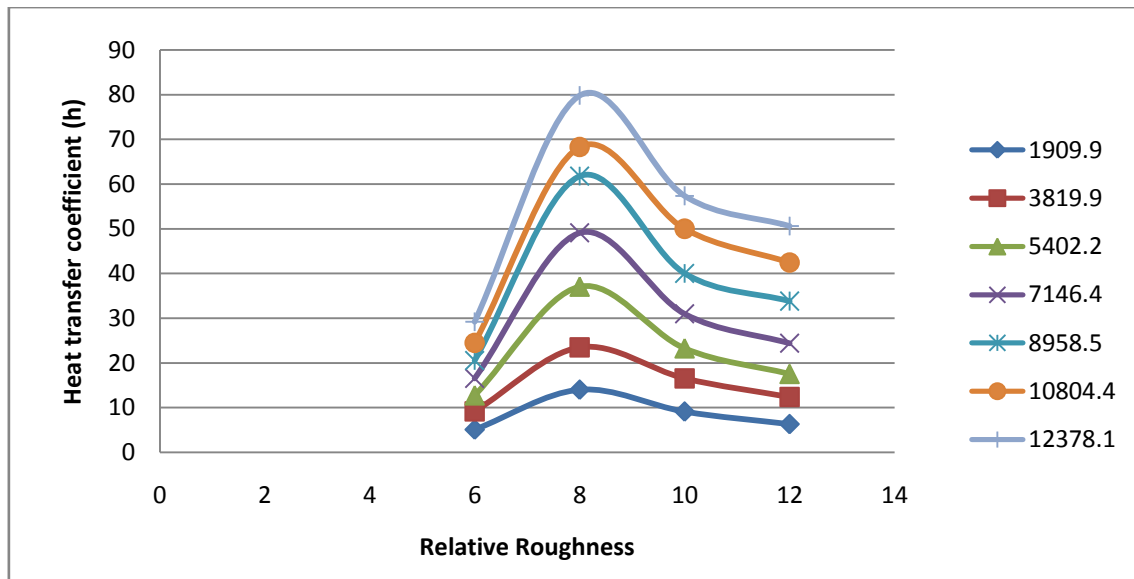


Fig .7. Heat Transfer Coefficient Vs Relative Roughness (P/e)

7. CONCLUSION

Based on experimental investigation following conclusion have been drawn:

1. Introduction of artificial roughness on under side of the absorber plate enhances Nusselt Number and Heat transfer coefficient compare to smooth duct.
2. Over the entire range of Reynolds Number, Nusselt Number increases and attains a maximum value at Relative Roughness of 8. It starts decreasing with increase in value of roughness.
3. Maximum enhancement of heat transfer coefficient occurs at Relative Roughness of 8 on either sides of it its value decreases.
4. Thermal efficiency of four roughened plates has been compared with the smooth duct. A plate with Relative Roughness of 8 gives maximum efficiency of 88.3%.
5. The Nusselt number for roughened duct is 3.7 times higher as compare to smooth duct under similar operating condition.

Nomenclature

A_c	surface area of absorber plate, m ²
B	half-length of full V-rib element, m
C_p	specific heat of air, J/kg K
d, d_o	print diameter of dimple/protrusion or geometric parameter of broken rib, m
D, Dh	equivalent or hydraulic diameter of duct, m
e	rib height, m
g	groove position, m
h	heat transfer coefficient, W/m ² K
H	depth of air duct, m

I	intensity of solar radiation, W/m ²
K	thermal conductivity of air, W/m K
L	length of test section of duct or long way length of mesh, m
m	mass flow rate, kg/s
P	pitch, m
DP	pressure drop, Pa
q _u	useful heat flux, W/m ²
Q _u	useful heat gain, W
Q _l	heat loss from collector, W
Q _t	heat loss from top of collector, W
S	length of discrete rib or short way length of mesh, m
T _o	fluid outlet temperature, K
T _i	fluid inlet temperature, K
T _a	ambient temperature, K
T _{pm}	mean plate temperature, K
T _{pm}	mean air temperature, K
U _L	overall heat loss coefficient, W/m ² K
v	velocity of air in the duct, m/s
w	width of rib, m
W	width of duct, m

Dimensionless parameters

B/S	relative roughness length
d/W	relative gap position
e ⁺	roughness Reynolds number
e/D, e/Dh	relative roughness height
e/H	rib to channel height ratio
f	friction factor
f	average friction factor
F _R	heat removal factor
g/e	relative gap width
g/P	relative groove position
G	momentum heat transfer function
L/e	relative long way length of mesh
l/s	relative length of metal grit
Nu	Nusselt number
N _{us}	Nusselt number for smooth channel
N _{ur}	Nusselt number for rough channel
N _{uav}	area-averaged Nusselt number
N _{uo}	Nusselt number for fully developed flow smooth channel
p/e	relative roughness pitch
Pr	Prandtl number
R	roughness function
Re	Reynolds number
St	Stanton number
St	average Stanton number
S/e	relative short way length of mesh
W/H	duct aspect ratio

Greek symbols

ϕ	rib chamfer/wedge angle, degree
η_{th}	thermal efficiency
η_{eff}	effective thermal efficiency
μ	dynamic viscosity, Ns/m^2
ρ	density of air, kg/m^3
α	angle of attack, degree
$(\tau\alpha)_e$	effective transmittance-absorptance product

REFERENCES

- [1] Hollands KGT, Shewan EC Optimization of flow passage geometry for air heating, plate-type solar collectors. Transactions of ASME, Journal of Solar Energy Engineering 1981; 103:323–30.
- [2] Choudhury C, Garg HP. Design analysis of corrugated and flat plate solar air heaters. Renewable Energy 1991; 1(5/6):595–607.
- [3] Hachemi A. Thermal performance enhancement of solar air heaters, by fan blown absorber plate with rectangular fins. Energy Research 1995; 19(7):567–78.
- [4] Yeh HM, Ho CD, Hou JZ The improvement of collector efficiency in solar air heaters by simultaneously air flow over and under the absorbing plate. Energy 1999; 24(10):857–71.
- [5] Hegazy AA Performance of flat plate solar air heaters with optimum channel geometry for constant/variable flow operation. Energy Conversion and Management 2000; 41(4):401–17.
- [6] Yeh HM, Ho CD, Lin CY. Effect of collector aspect ratio on the collector efficiency of upward type baffled solar air heaters. Energy Conversion and Management 2000; 41(9):971–81.
- [7] Zaid AA, Messaoudi H, Abenne A, Ray ML, Desmons JY, Abed B. Experimental study of thermal performance improvement of a solar air flat plate collector through the use of obstacles: application for the drying of “yellow onion”. Energy Research 1999; 23(12):1083–99.
- [8] Moummi N, Ali SY, Moummi A, Desmons JY Energy analysis of a solar air collector with rows of fins. Renewable Energy 2004; 29(13):2053–64.
- [9] Mohamad AA High efficiency solar air heater. Solar Energy 1997; 60(2):71–6.
- [10] Ramadan MRI, El-Sebaei AA, Aboul-Enein S, El-Bialy E. Thermal performance of a packed bed double-pass solar air heater. Energy 2007; 8:1524–35.
- [11] Pongjet Promvonge. Heat transfer and pressure drop in a channel with multiple 60° V-baffles; International Communications in Heat and Mass Transfer 37 (2010) 835–840.
- [12] Karwa RK. Experimental studies of augmented heat transfer and friction in asymmetrically heated rectangular ducts with ribs on heated wall in transverse, inclined, v-continuous and v-discrete pattern. Int Commun Heat Mass Transfer 2003; 30:241–50.
- [13] Saini SK, Saini RP. Development of correlations for Nusselt number and friction factor for solar air heater with roughened duct having arc-shaped wire as artificial roughness. Solar Energy 2008; 82:1118–30.

- [14] Bhagoria JL, Saini JS, Solanki SC. Heat transfer coefficient and friction factor correlations for rectangular solar air heater duct having transverse wedge shaped rib roughness on the absorber plate. *Renew Energy* 2002;25:341–69.
- [15] Jaurker AR, Saini JS, Gandhi BK. Heat transfer and friction characteristics of rectangular solar air heater duct using rib-grooved artificial roughness. *Solar Energy* 2006;80:895–7
- [16] Prasad BN, Saini JS. Effect of artificial roughness on heat transfer and friction factor in a solar air heater. *Solar Energy* 1988;41:555–60.(41).
- [17] Prasad BN, Saini JS. Optimal thermohydraulic performance of artificially roughened solar air heaters. *Solar Energy* 1991;47:91–6.(40).
- [18] Sahu MM, Bhagoria JL. Augmentation of heat transfer coefficient by using 90 broken transverse ribs on absorber plate of solar air heater. *Renew Energy* 2005;30:2057–63